Journal of Magnetism and Magnetic Materials 323 (2011) 3162–3167

Contents lists available at ScienceDirect

Journal of Magnetism and Magnetic Materials

journal homepage: www.elsevier.com/locate/jmmm

Transmission fingerprints in quasiperiodic magnonic multilayers

I.P. Coelho [a,c], M.S. Vasconcelos [b], C.G. Bezerra [c,*]

[a] Departamento de Ensino Superior, Instituto Federal de Educação, Ciência e Tecnologia do Maranhão, Imperatriz-MA 65919-050, Brazil
[b] Escola de Ciências e Tecnologia, Universidade Federal do Rio Grande do Norte, Natal-RN 59072-970, Brazil
[c] Departamento de Física, Universidade Federal do Rio Grande do Norte, Natal-RN 59072-970, Brazil

ARTICLE INFO

Article history:
Received 21 March 2011
Received in revised form
30 June 2011
Available online 12 July 2011

Keywords:
Ferromagnetic material
Magnonic multilayer
Spin wave
Quasicrystal

ABSTRACT

In this paper we investigated the influence of mirror symmetry on the transmission spectra of quasiperiodic magnonic multilayers arranged according to Fibonacci, Thue–Morse and double period quasiperiodic sequences. We consider that the multilayers composed of two simple cubic Heisenberg ferromagnets with bulk exchange constants J_A and J_B and spin quantum numbers S_A and S_B, respectively. The multilayer structure is surrounded by two semi-infinite slabs of a third Heisenberg ferromagnetic material with exchange constant J_C and spin quantum number S_C. For simplicity, the lattice constant has the same value a in each material, corresponding to epitaxial growth at the interfaces. The transfer matrix treatment was used for the exchange-dominated regime, taking into account the random phase approximation (RPA). Our numerical results illustrate the effects of mirror symmetry on (i) transmission spectra and (ii) transmission fingerprints.

1. Introduction

In the past two decades extensive theoretical and experimental investigations have been carried out for collective excitations of artificially layered systems. These specimens, composed of a wide variety of constituent materials, form an intriguing class of physical structures whose macroscopic properties are subject to design and control by varying the thickness and composition of the layers. Most of the initial studies concentrated on the properties of perfectly periodic structures. However, the discovery of quasicrystal by Shectman and co-workers [1] in 1984 aroused a great interest in quasiperiodic systems. This new kind of layered structure has attracted considerable attention in the past few years. Quasiperiodic systems display a degree of disorder that can be defined as an intermediate state between an ordered crystal (their definition and construction follow purely deterministic rules) and a disordered solid (many of their physical properties exhibit an erratic-like appearance) [2–4]. From a theoretical perspective, many groups have conducted detailed studies on the spectra of a number of elementary excitations in quasiperiodic structures such as light propagation, phonons, electronic transmission, polaritons, etc. [5–7]. It is interesting that a highly fragmented fractal energy spectrum can be considered the basic signature of a quasiperiodic system. The origin of this fractality may be attributed to the long-range order induced by the unusual hierarchical structure of the quasiperiodic sequences used to construct the system. On the experimental side, Merlin and co-workers grew the first quasiperiodic superlattice in 1985, following the Fibonacci sequence, by means of molecular beam epitaxy (MBE) [8]. Moreover, Fibonacci quasiperiodic Fe/Cr multilayers were recently grown on MgO (1 0 0) using dc magnetron sputtering [9].

Studies in the research field called magnonics [10,11] may allow the development of new devices that control, generate and propagate information using magnons (quantum of the spin waves), in a similar way that photons are manipulated in photonic crystals [12]. Therefore, the perspective of new technologies based on magnonic frequency band gaps has attracted considerable attention in recent years [13–18]. These frequency band gaps, which are intrinsic properties of magnonic crystals, are the key to controlling magnon propagation and the basis of magnonics, whose range of applications varies from magneto-electronic devices [16] to magnonic waveguides [18]. Therefore, the application of new geometries and arrangements in magnonic systems may affect the profile of magnonic band gaps, thereby opening new possibilities in magnonics [19].

On the other hand, it is known from the theory of continuous phase transitions that critical behavior depends only on global properties, namely the geometric dimension of the system and the symmetries of its order parameter. It is insensitive to differences in microscopic interactions between atoms or molecules. Thus, many systems that are distinct within a microscopic scale show the same critical behavior. It is therefore possible to classify several systems into a few universality classes. Although

* Corresponding author.
E-mail address: cbezerra@dfte.ufrn.br (C.G. Bezerra).

0304-8853/$ - see front matter © 2011 Elsevier B.V. All rights reserved.
doi:10.1016/j.jmmm.2011.07.003

we are not dealing here with critical properties, in quasiperiodic arrays a similar classification may be possible, depending on the quasiperiodic sequence applied to construct the structure. This is because each specific quasiperiodic sequence used to construct the system presents a specific degree of disorder, which emerges in the spectra (see for example Ref. [5]). For this reason a method was developed to distinguish spectral properties among quasiperiodic systems [20]. The method is based on calculating transmission spectra for several generations of a particular quasiperiodic sequence as a function of energy (or frequency). The transmission spectra, as expected, display self-similar behavior. The next step is to construct a return map T_{N+1} versus T_N, where T_N is the transmission probability corresponding to the Nth generation of the quasiperiodic structure. The return map provides a pattern (or attractor) that depends only on the specific quasiperiodic sequence applied in the construction of the quasiperiodic system. For this reason, the attractors were named fingerprints since they can promptly identify the quasiperiodic sequence associated to the physical system under consideration.

The method described above has been applied in the study of photonic quasiperiodic crystals [21] and quasiperiodic magnetic superlattices [22]. We recently extended these studies to include internal structural symmetry, or mirror symmetry, for one-dimensional photonic crystals [23]. In particular, we studied the effects of mirror symmetry on the transmittance spectra and return maps of light waves. The purpose of this paper is to gain better understanding of the effects of mirror symmetry on layered structures. More specifically, we investigated the effects of mirror symmetry on the transmittance spectra and return maps of spin waves propagating in magnetic multilayers constructed according to Fibonacci, double period and Thue–Morse quasiperiodic sequences. This paper is organized as follows. In Section 2 we discuss the algorithm used to construct the physical system and the calculation method, which is based on the transfer matrix approach. Section 3 is devoted to presenting our numerical results. Finally, our conclusion are summarized in Section 4.

2. Physical system

The geometry of the physical system is described in Fig. 1. We define the Cartesian axes in such a way that the z-axis is normal to the planes of the layers. The multilayer system is composed of slabs made of two Heisenberg ferromagnetic materials A and B stacked in a quasiperiodic array. Fig. 1 shows mirror symmetry around plane $z=L/2$, where L is the multilayer size. The multilayer structure is surrounded by two semi-infinite slabs of a third Heisenberg ferromagnetic material labeled material C. We consider the spins in the bulk and across the interfaces coupled by usual exchange coupling.

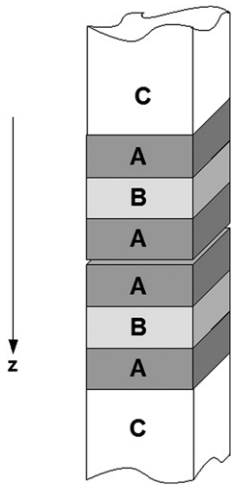

Fig. 1. Schematic representation of the third generation of a Fibonacci magnetic multilayer with mirror symmetry.

Let us now briefly describe the construction of the quasiperiodic sequences considered in this study. The Fibonacci sequence with mirror symmetry can be expressed as $S_N=L_NR_N$, where L_N is generated by the inflation rule $A\to AB$ and $B\to A$, while R_N is generated by the inflation rule $A\to BA$ and $B\to A$. Similarly, the Thue–Morse sequence with mirror symmetry can be expressed as $S_N=L_NR_N$, where L_N is generated by the inflation rule $A\to AB$ and $B\to BA$, while R_N is generated by $A\to BA$ and $B\to AB$. Finally, the double-period sequence with mirror symmetry can be represented as $S_N=L_NR_N$, where L_N is generated by an equivalent inflation rule $A\to AB$ and $B\to AA$, while R_N is generated by $A\to BA$ and $B\to AA$.

Although the model is described elsewhere, we will describe it again, for the reader's convenience, following the lines of Ref. [22]. In order to calculate the spin waves that can propagate in the aforementioned quasiperiodic structures, we consider the bulk exchange parameters as J_A, J_B and J_C and, for simplicity, we assume the same lattice constant a for each material. The exchange couplings at any interface $\alpha-\beta$ are $I_{\alpha\beta}$ (with α, β being A,B or C). The spins within each material are S_A, S_B and S_C, respectively. The Heisenberg Hamiltonian for the bulk of each specimen, in the absence of an external magnetic field and not considering any anisotropic exchange field, is given by

$$\mathcal{H}_\alpha=(-1/2)\sum_{i,j}J_\alpha\vec{S}_i\cdot\vec{S}_j, \tag{1}$$

where $\alpha=A$, B or C and the sum considers nearest neighbors i and j. The propagating spin wave is found from the operator $S_i^+=S_i^x+iS_i^y$, i.e.

$$i\hbar(\partial S_i^+/\partial t)=[S_i^+,\mathcal{H}]. \tag{2}$$

The spin wave amplitudes are given, within each material, by a linear combination of the positive- and negative-going solutions for each bulk medium, namely,

$$S_i^+=\{C\exp[i\vec{k}_C\cdot(\vec{r}-\vec{r}_C)]+C'\exp[-i\vec{k}_C\cdot(\vec{r}-\vec{r}_C)]\}\exp(-i\omega t) \tag{3}$$

in component C, and with analogous expressions (with C labels replaced by A and B) in components A and B, respectively. Here $\vec{r}_C$ is the origin of the material C at the interface. The above solutions must satisfy a matching condition at the interfaces given by

$$i\hbar(\partial S_i^+/\partial t)=\sum_{i,j}J_\alpha(S_jS_i^+-S_iS_j^+). \tag{4}$$

The boundary conditions are written in the matrix form, which can be represented, after some straightforward algebra, as (for details see Refs. [20–22])

$$\begin{bmatrix}C_1\\C_1'\end{bmatrix}=M_N\begin{bmatrix}C_2\\0\end{bmatrix}. \tag{5}$$

Here M_N is the transfer matrix associated to the Nth generation of the quasiperiodic multilayer under consideration. It connects the spin wave amplitudes of the upper semi-infinite slab (C_1,C_1') to the spin wave amplitudes of the lower semi-infinite slab $(C_2,0)$. Therefore, once we know the transfer matrix, reflectance and transmittance are given by the matrix elements as $R=|M_{21}/M_{11}|^2$ and $T=|1/M_{11}|^2$, respectively.

In fact, the transfer matrix is composed of the product of transmission and propagation matrices of each individual slab. For example, the transmission of a normal incident spin wave

across interfaces $\alpha \rightarrow \beta$ (α, β being A, B or C) is represented by the matrix

$$M_{\alpha\beta} = \begin{bmatrix} (I_{\alpha\beta}I_{\beta\alpha} - \overline{\lambda}_{\alpha\beta}\overline{\lambda}_{\beta\alpha})/[(\lambda_{\alpha\beta} - \overline{\lambda}_{\alpha\beta})I_{\beta\alpha}] & (I_{\alpha\beta}I_{\beta\alpha} - \overline{\lambda}_{\alpha\beta}\lambda_{\beta\alpha})/[(\lambda_{\alpha\beta} - \overline{\lambda}_{\alpha\beta})I_{\beta\alpha}] \\ (I_{\alpha\beta}I_{\beta\alpha} - \lambda_{\alpha\beta}\overline{\lambda}_{\beta\alpha})/[(\overline{\lambda}_{\alpha\beta} - \lambda_{\alpha\beta})I_{\beta\alpha}] & (I_{\alpha\beta}I_{\beta\alpha} - \lambda_{\alpha\beta}\lambda_{\beta\alpha})/[(\overline{\lambda}_{\alpha\beta} - \lambda_{\alpha\beta})I_{\beta\alpha}] \end{bmatrix}, \tag{6}$$

while the propagation of the spin wave within a certain slab γ ($\gamma = A$ or B) is represented by the matrix

$$M_{\gamma} = \begin{bmatrix} \overline{t}_{\gamma} f_{\gamma} & 0 \\ 0 & t_{\gamma} \overline{f}_{\gamma} \end{bmatrix}. \tag{7}$$

The elements of the two above matrices are described in Ref. [22]. It is worthwhile to remark that these matrices are completely analogous to the matrices of Ref. [21].

3. Numerical results

Here we will present some numerical results for the transmission probability of magnetic quasiperiodic structures with mirror symmetry. We assumed that the number of monolayers in each slab to be $n_A = n_B = 4$ (see Ref. [22]). Since the size of these systems grows exponentially, as generation index N increases, the transmittance goes to zero very quickly. In order to circumvent this difficulty, we calculate maximum generation index N, for which the transmittance is less than 10^{-12}, versus reduced frequency Ω. Therefore, the maximum generation index is an indirect measurement of the transmission probability for the spin waves. Fig. 2(a) shows the plot of maximum generation number N versus reduced frequency $\Omega = \hbar\omega/J_A S_A$ for the Fibonacci multilayer system in the frequency range $1.800 < \Omega < 1.855$. The largest generation number attained was $N = 64$. From there, we can observe several dips and peaks forming band gaps in the frequency. These band gap regions, which correspond to more localized states in higher orders of the Fibonacci multilayer system, exhibit self-similar properties. The self-similarity is illustrated in Fig. 2(b) and (c), which shows the same spectra as in Fig. 2(a), but with other frequency scales. The arrows in the figures indicate the scaling points where self-similarity occurs. Fig. 2(b) and (c) shows that the band gaps obey a hierarchical frequency distribution centered around $\Omega \approx 1.829$.

In Fig. 3(a) we plot the maximum generation number N versus reduced frequency Ω for the Thue–Morse multilayer system in the frequency range $4.6711 < \Omega < 4.67658$. The maximum generation number achieved was $N = 100$. As in the Fibonacci case, we observe several band gaps in this frequency range. They also have self-similar properties, as shown in Fig. 3(b) and (c). The arrows in these figures indicate the scaling points where the self-similarity is most evident, i.e., around $\Omega \approx 4.6765$.

The double-period multilayer case is shown in Fig. 4(a), where we plot N versus reduced frequency Ω in the range $0.142 < \Omega < 0.167$. As in the previous cases, we have several band gaps hierarchically distributed in this frequency range. The largest generation number was $N = 56$. Self-similarity can be observed in Fig. 4(b) and (c). The arrows in the figures indicate the scaling points. However, in contrast to Fibonacci and Thue–Morse cases, the scaling points are not located in the same frequency region. In Fig. 4(a) the scaling points delimit the frequency region $0.15433 < \Omega < 0.1566$, while in Fig. 4(b) the scaling points delimit the frequency region $0.1570 < \Omega < 0.1576$.

Before concluding, we should discuss the return maps, without which our analysis would not be complete. In fact, the study of return maps is very useful in determining the influence of mirror

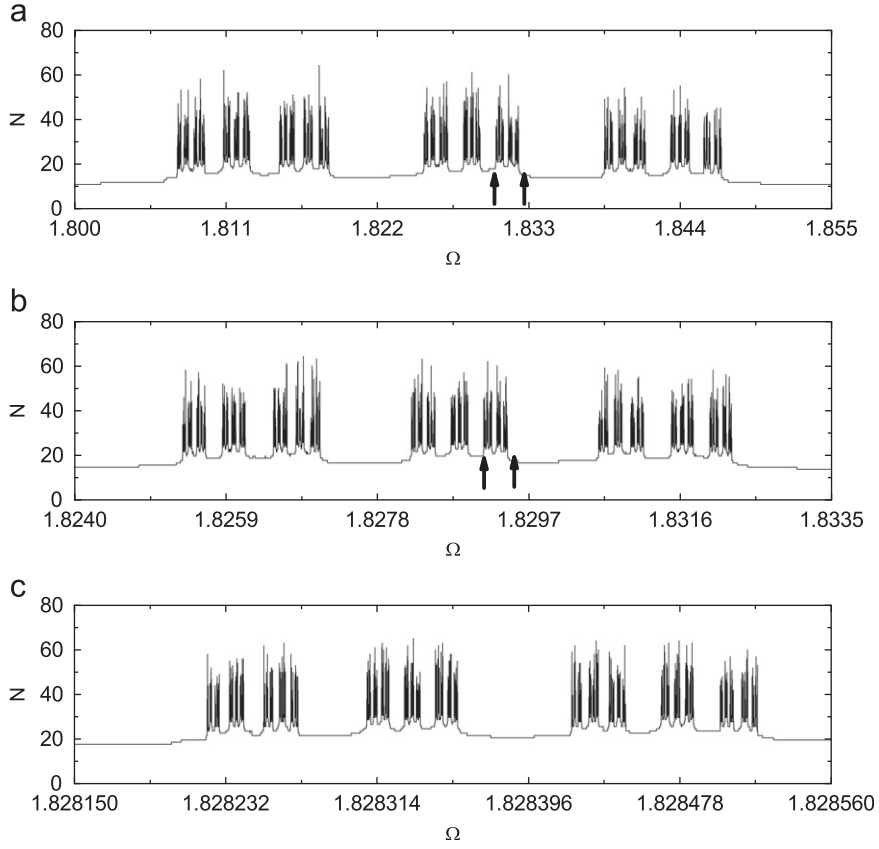

Fig. 2. Maximum generation index N versus reduced frequency Ω for a Fibonacci multilayer with mirror symmetry in three different frequency ranges: (a) $1.800 < \Omega < 1.855$, (b) $1.8240 < \Omega < 1.8335$ and (c) $1.82815 < \Omega < 1.82856$.

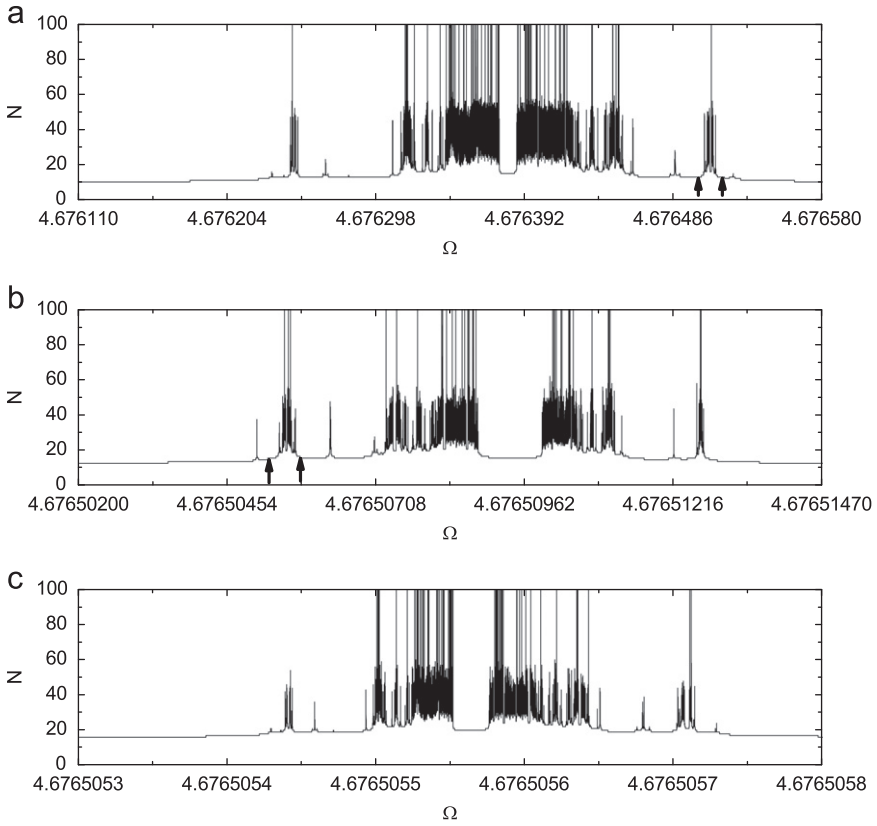

Fig. 3. Maximum generation index N versus reduced frequency Ω for a Thue–Morse multilayer with mirror symmetry in three different frequency ranges: (a) $4.67611 < \Omega < 4.67658$, (b) $4.676502 < \Omega < 4.676514$ and (c) $4.6765053 < \Omega < 4.6765058$.

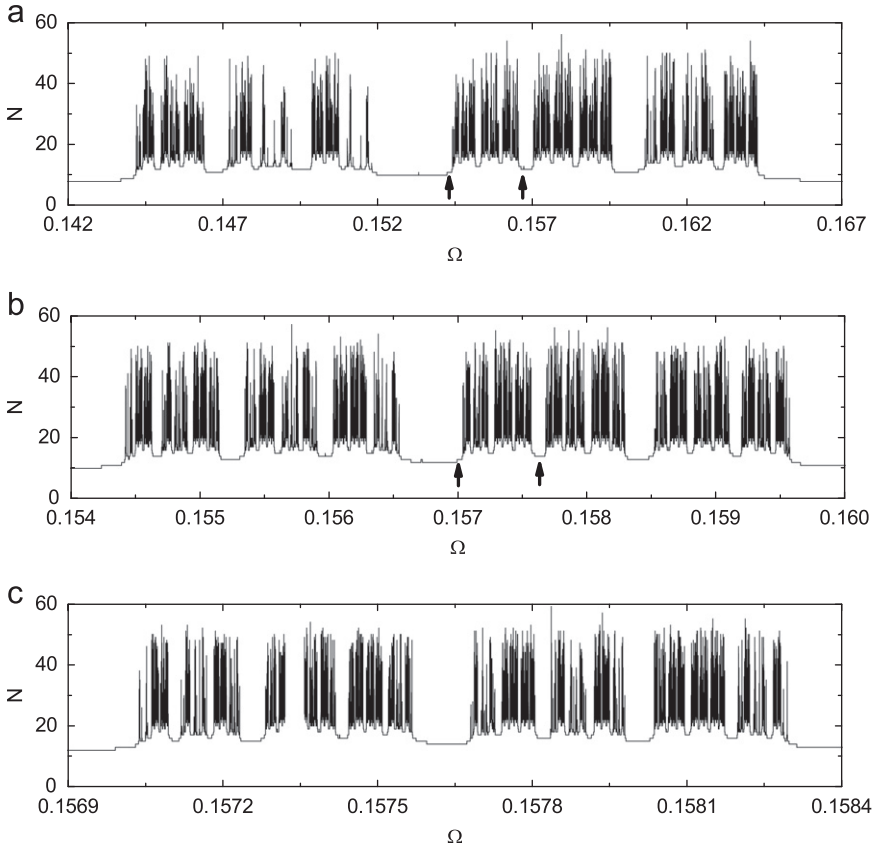

Fig. 4. Maximum generation index N versus reduced frequency Ω for a double-period multilayer with mirror symmetry in three different frequency ranges: (a) $0.142 < \Omega < 0.167$, (b) $0.154 < \Omega < 0.160$ and (c) $0.1569 < \Omega < 0.1584$.

structure on quasiperiodic magnetic multilayers. We can physically understand the return maps as analogous to attractors of a time series, generated by some deterministic dynamic evolution. Return maps T_{N+1} versus T_N can be constructed after we generate the series $T_1,T_2,T_3,\ldots,T_N,\ldots$ of transmission probabilities corresponding to larger and larger sequences $S_1,S_2,S_3,\ldots,S_N,\ldots$, for a single frequency Ω. We choose the frequencies in such a way that we obtain non-zero transmission for high generation indexes N. For the quasiperiodic magnetic structures considered in this work, the deterministic inflation rules induce long-range correlations that are reflected in the spectra and, as a consequence, in the return maps through the return map's pattern. Although the pattern of the return map cannot be determined *a priori*, it depends only on the degree of disorder of each quasiperiodic structure [20].

Fig. 5 shows the return maps for the spin wave transmittance spectra studied here. As cited previously, we chosen frequency values corresponding to high transmittance, so that high generation indexes N could be achieved. Fig. 5(a) shows the return map for the Fibonacci multilayer with reduced frequency $\Omega = 0.5335$.

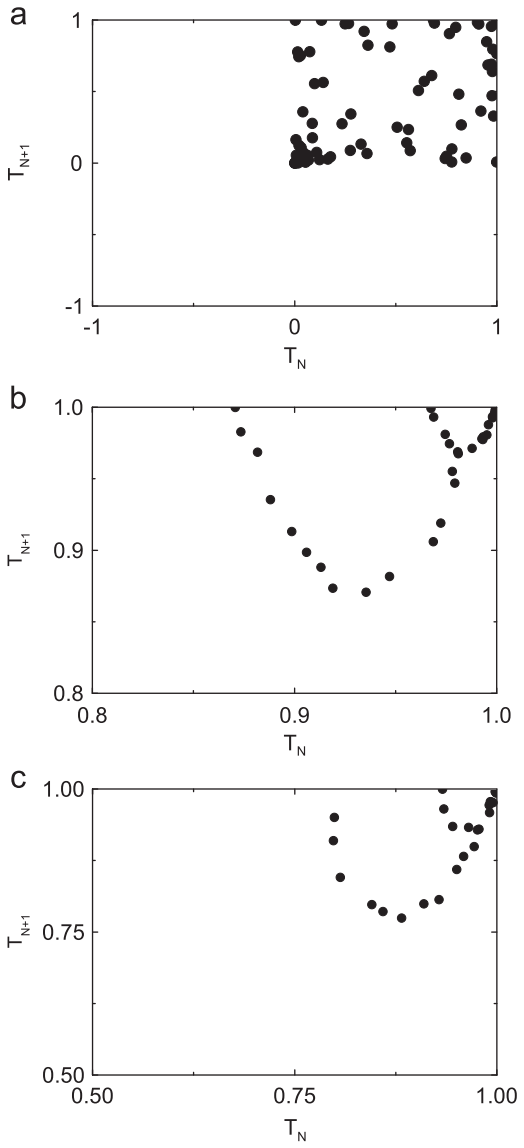

Fig. 5. The return map T_{N+1} versus T_N illustrating the fingerprint of magnetic quasiperiodic structures with mirror symmetry: (a) Fibonacci, (b) Thue–Morse and (c) double-period.

The return map is delimited by a box whose vertices are defined by $0.001 > T_N > 1.0$ and $0.001 > T_{N+1} > 1.0$. A similar pattern was found in the previous studies on quasiperiodic layered systems [21–23]. Our numerical result shows that mirror symmetry does not affect the return map for the Fibonacci case. In Fig. 5(b) we show the return map for Thue–Morse quasiperiodic magnetic multilayer with reduced frequency $\Omega = 0.000062$. The pattern in the return map is similar to two parabolas, and it is different from the return maps obtained for Thue–Morse quasiperiodic magnetic multilayers without mirror symmetry, which show just one parabola [22]. On the other hand, it is similar to the return map obtained for Thue–Morse quasiperiodic photonic multilayers with mirror symmetry, which exhibits a pattern with two parabolas [23]. Finally, the return map for the double-period quasiperiodic magnetic multilayers with mirror symmetry is shown in Fig. 5(c). The pattern was obtained considering reduced frequency $\Omega = 0.0000249$. As in the Thue–Morse case, the return map corresponds to two parabolas and it is different from the return map obtained for double period quasiperiodic magnetic multilayers without mirror symmetry, but similar to the return map obtained for double period quasiperiodic photonic multilayers with mirror symmetry [23]. We can infer, from the numerical results described, that mirror symmetry had an effect mainly on the Thue–Morse and double-period transmission spectra, with the emergence of a two parabolas pattern in the return maps. The same result was recently found for quasiperiodic photonic multilayers with mirror symmetry [23].

4. Conclusions

In conclusion, we studied the transmission spectra of spin waves that can propagate in quasiperiodic magnetic multilayers constructed according to Fibonacci, double period and Thue–Morse quasiperiodic sequences with mirror symmetry. Our numerical results show a beautiful self-similar behavior, with well-defined scaling points in the plot of maximum generation index N versus reduced frequency Ω, which reveals the presence of fractality in frequency band gaps distribution (see Figs. 2–4). It is known that the definition or inflation rules of these sequences impose long-range correlations on the layers. The pattern of return map T_{N+1} versus T_N reflects these long-range correlations. We can conclude from our numerical results that mirror symmetry, compared to the case without mirror symmetry [22], (i) has no effect on the return maps for the Fibonacci case but (ii) it does have effect on the return maps for the Thue–Morse and double period cases. Finally, comparing these results to the return maps found for quasiperiodic photonic multilayers [23], we observe a strict similarity pattern, reinforcing the idea that return maps depend basically on the quasiperiodic sequence used to construct the physical system under consideration.

Acknowledgments

This work was partially financed by the Brazilian Research Agencies CAPES, CNPq, FINEP and FAPEMA.

References

[1] D. Shechtman, I. Blech, D. Gratias, J.W. Cahn, Phys. Rev. Lett. 53 (1984) 1951.
[2] P.J. Steinhardt, S. Ostlund, The Physics of Quasicrystals, World Scientific, Singapore, 1987.
[3] C. Janot, Quasicrystals: A Primer, Oxford University Press, Oxford, 1993.
[4] M. Senechal, Quasicrystals and Geometry, Cambridge University Press Cambridge, 1995.
[5] E.L. Albuquerque, M.G. Cottam, Polaritons in Periodic and Quasiperiodic Structures, Elsevier, Amsterdam, 2004.

[6] C.G. Bezerra, E.L. Albuquerque, Physica A 245 (1997) 379.
[7] C.G. Bezerra, M.G. Cottam, Phys. Rev. B 65 (2002) 054412.
[8] R. Merlin, K. Bajema, R. Clarke, F.-Y. Juang, P.K. Blattacharya, Phys. Rev. Lett. 55 (1985) 1768.
[9] T. Freire, C. Salvador, M.A. Correa, C.G. Bezerra, C. Chesman, A.B. Oliveira, F. Bohn, Solid State Commun, 151 (2011) 337.
[10] Z.K. Wang, V.L. Zhang, H.S. Lim, S.C. Ng, M.H. Kuok, S. Jain, A.O. Adeyeye, ACS Nano 4 (2010) 643.
[11] K.S. Lee, D.S. Han, S.K. Kim, Phys. Rev. Lett. 102 (2009) 127202.
[12] J.D. Joannopulos, S.G. Johnson, J.N. Win, R.D. Meade, Photonic Crystals: Molding the Flow of Light, Princeton University Press, Princeton, 2008.
[13] M. Krawczyk, H. Puszkarski, Phys. Rev. B 77 (2008) 054437.
[14] V.V. Kruglyak, R.J. Hicken, J. Magn. Magn. Mater. 306 (2006) 191.
[15] S.A. Nikitov, C.S. Tsai, Y.V. Gulyaev, Y.A. Filimonov, A.I. Volkov, S.L. Vysotskii, P. Tailhades, Mater. Res. Soc. Symp. Proc. 834 (2005) 87.
[16] H. Xi, X. Wang, Y. Zheng, P.J. Ryan, J. Appl. Phys. 105 (2009) 07A502.
[17] S. Neusser, D. Grundler, Adv. Mater. 21 (2009) 2927.
[18] A. Kozhanov, D. Ouellette, Z. Grith, M. Rodwell, A.P. Jacob, D.W. Lee, S.X. Wang, S.J. Allen, Appl. Phys. Lett. 94 (2009) 012505.
[19] A.V. Chumak, A.A. Serga, S. Wolff, B. Hillebrands, M.P. Kostylev, J. Appl. Phys. 105 (2009) 083906.
[20] P.M.C. Oliveira, E.L. Albuquerque, A.M. Mariz, Physica A 227 (1996) 206.
[21] M.S. Vasconcelos, E.L. Albuquerque, Phys. Rev. B 59 (1998) 11128.
[22] C.G. Bezerra, M.S. Vasconcelos, E.L. Albuquerque, A.M. Mariz, Physica A 329 (2003) 91.
[23] I.P. Coelho, M.S. Vasconcelos, C.G. Bezerra, Phys. Lett. A 374 (2010) 1574.